

# Bond Graph Modeling and Control of Induction Motor used in Ladle Cranes

Abhijit Roy, Prof. Anup Kumar Saha

Department of Mechanical Engineering, National Institute of Technology Durgapur, Durgapur - 713209, India

**Abstract**—Initially when power is supplied, induction motor runs at its rated speed with the recommended specifications and varying applications. Control of the motor's speed with the improvement of the induction motor's dynamic and steady state characteristics which are non-linear in nature, has been possible due to the advancement of electronics. The popularity of this motor has resulted into lot of research including the transient behavior of the motor. A methodology based on modeling capabilities along with control and its computer simulation has been proposed in this paper and is represented by dynamic modeling of three-phase four pole induction motor. When physical modeling of systems is necessary the bond graph approach is good, again it is also a good tool for combining different energy domains. Dependencies between different components can easily be found through the method of bond graph. This study was conducted on the basis of parameters collected from different ladle cranes motors of Durgapur Steel Plant in India.

**Keywords**— **Bond graph, Controller, Induction motor, Ladle Crane, Modeling, Simulation.**

## I. INTRODUCTION

An induction machine or a synchronous machine comprises of a magnetic circuit and interlinked with two electric circuits. As transmission of power by electromagnetic induction from one circuit to another, thus are called induction machines. In induction motor termed as induction machine, electric power converted into mechanical power. Stator of motor is connected to the power source and current induced on the rotor is connected to secondary winding. Converting electric energy to mechanical energy is performed by different motors, of which Induction motors are extensively used in industry- particularly in steel sector due to their ruggedness and simplicity and about 90% of industrial motors are induction motors [6]. Slip ring induction motor as shown in Fig.1 preferred to the squirrel cage motor as one more degree of freedom for starting & speed control. Slip ring Induction Motor is the first choice where high starting torque & variable speed is required, or where heavy load during start. The hoist & lowering operation is difficult to understand as smooth operation

over a wide speed range for raising or lowering the hook at controlled speeds irrespective of the variation of ladle weight. During lifting, motoring torque with a relatively flat speed/torque characteristic by the drive is necessary to prevent motor's excessive speed change from full load to empty ladle conditions. Depending upon whether the load torque exceeds the mechanical friction of the hoist mechanism during lowering, the drive torque can be monitoring or braking. On releasing the mechanical brake, motoring torque is being provided by the motor to exceed friction, but the motor must change to a braking mode instantly as the load torque exceeds the running friction. For smooth start and control speed resister controllers in the rotor circuit of Induction Motor are used. By insertion of relatively simple passive frequency sensitive networks, certain desired torque speed characteristics can be achieved.

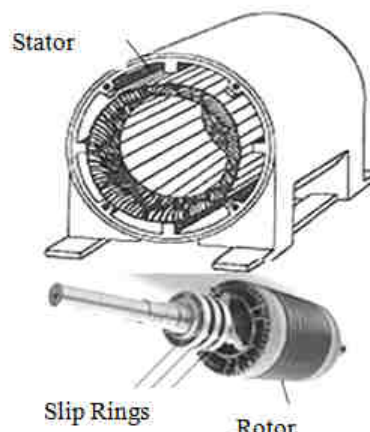


Fig. 1: View of a ladle crane Hoist induction motor

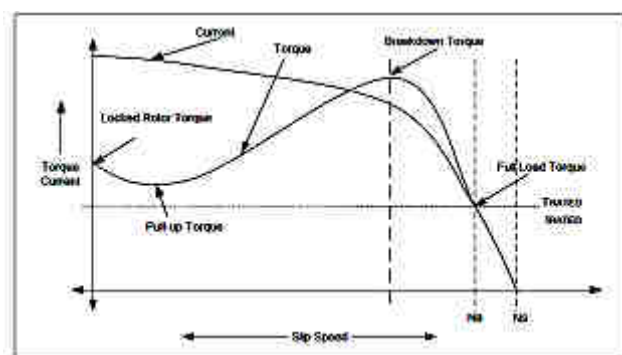


Fig. 2: Speed-torque characteristics of IM

Highly reduced starting current and improved torque current ratio can be achieved through careful selection of network. To study the effect of rotor impedance on the performance of Induction Motors is necessary to understand the industrial systems incorporating the Slip ring Induction Motors. Larger space, poor efficiencies, slow speed etc., were the limitations for variable speed drives but, the power electronics made it possible of variable speed drive in smaller size, high efficiency along with high reliability [1]. In modern control methods state space techniques are being used and modern power electronic devices have been realized the drive stabilizing method along with its improvement in transient responses [2]. Advanced control of induction machines is so important but not so simple. Different methods have been proposed so far for the control of induction motors [3]. However, the family of mathematical models with concentrated parameters comprises different approaches but two of them are more popular: *the phase coordinate* model and the *orthogonal (dq)* model [4]. Speed control required for allowing soft starting and stopping of the travel motions of ladle crane for enabling its correct positioning of load. For the lifting and lowering drive, the speed control in a wide speed range, from zero to nominal values, is required. Because of the precision when rising and lowering ladle, the possibility of working at a very low speed and hold the ladle in the standstill is required, without using the mechanical brakes. The torque and power that have to be delivered by the drive may be obtained from the torque versus speed characteristic as shown in Fig.2 from the load (so-called mechanical characteristics) and the differential equation of motion, (Belmans et al., 1993; Mitrovic et al., 2011)[5].

The goal of this research is to present the physical model of the motor and to develop a bond graph models, in order to obtain a unified approach on modeling of the induction machines for control purposes , adopting an innovative matter of opinion that emphasize the control aspects—in lieu of the classical electrical engineering viewpoint. Simulation for the dynamic performance of an induction motor model is done by Bond graph approach. This simulated program makes it easy to understand the development process. From a control theory perspective the review can be done again. The literature review reflects a close relation between this classical technique with that of moribund ideas [7]. Standard assumptions were made during physical modeling of the induction motor but control of the machine were in a matter of opinion.

## II. PHYSICAL MODEL

An electrical rotating machine generally consists of three distinct physical structures – a stationary iron with

winding and a rotating iron with winding on a rigid shaft coupled to a drive. Thus three distinct energy port stator, rotor and shaft can be identified in a rotating machine. The three ports exchange energy with environment and between themselves and this exchange takes place in the air gap.

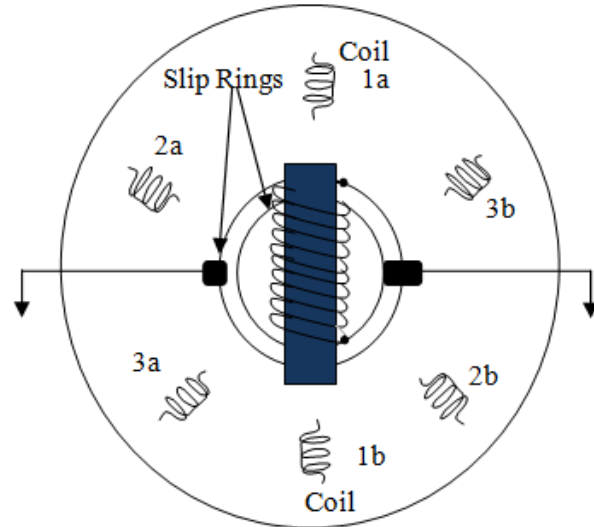


Fig. 3: A 3-phase 4-pole motor coil distribution stator

As the rotor never runs in synchronous speed with the stator poles, slip ring induction motors are called asynchronous motor. Both the squirrel cage and slip ring induction motor has same stator construction but main difference is that slip ring induction motors usually have a “Phase-Wound” rotor. The stator contains multiple distinct windings per motor pole, driven by corresponding time shifted sine waves in polyphase motors. In practice, this is two or three phases. A 3-phase, double-layer, distributed winding consisting of coils in alternators are used in these rotors. The rotor core has slots to accommodate formed 3-single phase windings placed 120 degrees phase apart, is made up of steel laminations. If the stator is wound for less than 3-phase the rotor is wound for identical numbers of poles as in the and is always 3-phase. These three windings are “starred” internally and the other end to three insulated slip-rings mounted on the rotor shaft. With the help of carbon brushes, held against the rings by spring assembly, the three terminal ends touch these three slip rings and are further connected externally to a 3-phase start connected rheostat. The combination of slip ring and external rheostat helps to add external resistance to the rotor circuit, which on the other hand enables them to have a higher resistance during starting and thus higher starting torque.

In a 3-phase 4-pole induction machine the two symmetrical ( $a, b, c$ )-windings arrangement, for stator (subscript s) and rotor (subscript r), are shown in Fig.3 and Fig.5. Assumptions made during formulation that

these are in magnetic linearity whose axes are  $120^\circ$  apart from each other and ideal sinusoidally wound coils, with phase resistances  $R_{s,r}$  with equivalent number of turns  $N_{s,r}$ . The variables considered on the electromagnetic magnitudes on each of these axes are known as machine variables. For a 4-pole machine, the electrical rotor speed  $\omega_r$  shown in the figure coincides with the actual rotor speed, i.e.,  $\omega = \omega_r$ , and the rotor instantaneous angular position is  $\theta = \theta_r = \omega_r dt$ . For the general case of a machine with  $P$  poles or, equivalently,  $np = P/2$  pole pairs, the general relationships are as given below:

$$\omega = \omega_r/np \quad \text{and} \quad \theta = \theta_r/np$$

The slip rings running normally are short-circuited by a metal collar, which is inserted along the shaft enables the three rings touch each other. To avoid frictional losses, wear and tear, the brushes are generally lifted from the slip-rings. Under normal running conditions, the wound rotor and squirrel cage rotor acts identically. From the motor's physical construction the torque-speed relationship will be examined and subsequently magnetic field behavior and general equation for torque as a function of slip will be derived from the per-phase equivalent circuit of a 3-phase induction motor as shown in the Fig.4 below. To prevent saturation the V/f ratio must not exceed that of rated voltage and frequency. Even at fully loaded condition motor must not exceed this ratio for any period of time. The equivalent circuit of the motor at Fig.4 shows that the magnetizing current ( $I_m$ ) producing the flux is a shunt component across the incoming supply and is not really affected by load. It is common, however, to operate the motor at lower flux under reduced-load conditions and that way to lower energy consumption and motor heat. The power crossing the terminals 'AB' in Fig.4 is the difference of electrical power input per phase to that of stator copper loss and iron loss. Thus it is the power that is transferred through the air gap from the stator to the rotor, known as the power across the air gap.  $R_r(1 - s)/s$  is the resistance equivalent to the power which is converted to mechanical power output or useful power and  $L_m$  is the magnetizing reactance of the winding.

Table.1: Parameters of Induction Motor

Description	Value
RMS value of supply voltage (line)	415
Number of poles	4
Stator coil resistance	0.550 ohm
Equivalent rotor coil resistance	0.568 ohm
Mutual inductance	0.1000 H
Stator coil inductance	0.0048 H
Rotor coil inductance	0.0025 H

There are two conditions of rotor speed determination of induction motor. It is at no load condition when rotating

speed of rotor is near to synchronous speed and when the rotor speed falls it is on-load condition. Relative motion between rotor and magnetic field at no-load position is very small, and the rotor frequency is also very small resulting maximum rotor current flow as the reactance of the rotor is nearly zero. On the other hand with the increases of the motor's load, its slip increases and since the rotor slip is larger, the rotor frequency rises, resulting minimum rotor current flow as the reactance of the rotor is very high overall induced torque increases to supply the motor's increased load.

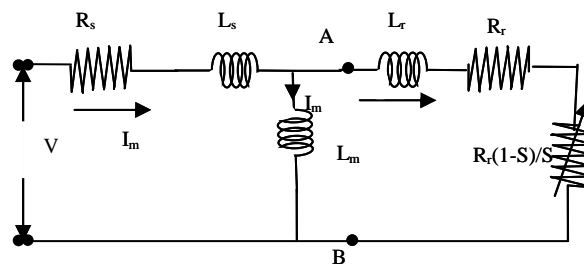


Fig 4: Equivalent Circuit of 3 phase induction Motor

### III. DIFFERENT METHODS TO CONTROL THREE PHASE INDUCTION MOTORS

The three speed of an induction motor are controlled by following different methods as under:

- a. Vector Control method
- b. By Constant V/f control method
- c. By Variable rotor resistance control method
- d. By Variable supply voltage control method
- e. By Variable Supply Frequency method
- f. By Slip recovery method
- g. By Pole Changing

The torque slip relation for an Induction Motor with external rotor impedance can be obtained from above equation. Now let us observe the effect for different network parameters.

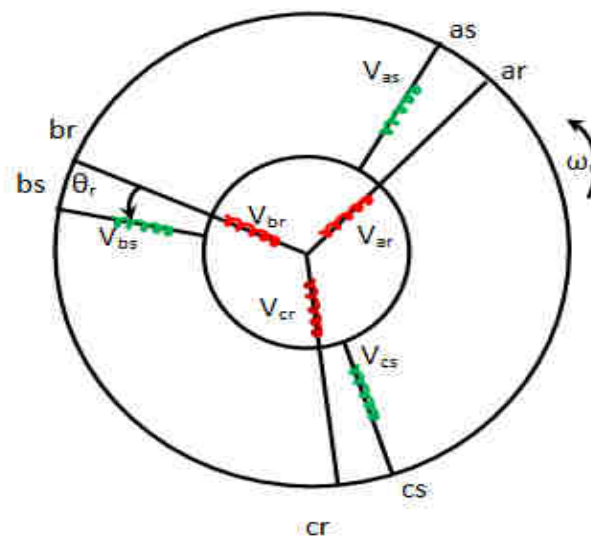


Fig. 5: A 3-phase 4-pole 120 degrees phase apart

#### IV. BOND GRAPH MODELING

Bond Graph, a graphical modeling tool preserves the computational and contour structure of the system to be modeled. The cause and effect diagram of the system can easily be achieved by Bond Graph users. Power flow throughout the system can be obtained from this methodology. Model subsystems of different domain can easily be connected by Bond Graphs and at the same time concise meaningful and larger mixed-domain models can be generated. Power flows and signal flow information across the same energy domain boundaries in Bond Graph form the cause and effect relationships within interdisciplinary systems.

An induction motor can easily be treated as a transformer with its primary winding considered to be stationary but the secondary is free to rotate. The air gap between the rotor and the stator through which the flux passes is the major difference with transformer. In this section model of induction motor along with open loop control developed, useful for purpose of simulation. Handling analytically of these models is easier almost similar to synchronous machines. Induction machines can act as high performance servomotors due to latest development in power electronics and control technology.

The performance of a dc machine in which torque is a

simple function of applied current can be imitated. For a single field winding machine, this can be expressed as,

$$T = GI_f I_a$$

Once the desired torque is known it makes the control of such a machine quite easy as it translates that torque command into a current and the motor does the rest. In servo applications of induction motor it was thought to be “hard to control”. Not too much effort is needed and even little computation needed to control correctly, but this is becoming increasingly trinket. In DC motors, rotor receives power by conduction but in case of AC motors, power received by induction. The induction is similar to the secondary side of a two winding transformer which receives its power from primary. Comparing induction motor with a transformer, the primary winding is stationary and that of the secondary is free to rotate. The air gap between the rotor and the stator through which the flux passes is the only major difference. We will discuss about the model of a three-phase four-pole basic induction motor as given in *Fig. 6*.

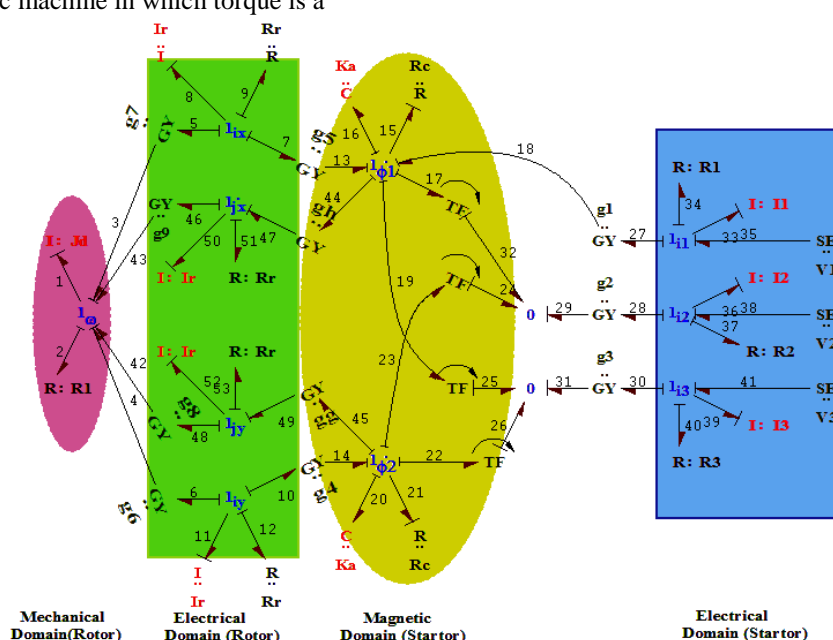


Fig. 6: Bond graph Sub model of three phase four pole induction motor used in Ladle Crane

The magnetic circuit point potentials at various joints are suffixed with various 0-junctions and one such 0-junction has been taken as ground. The C-elements in Fig. 6 of the sub model indicates various reluctances. Again the reluctance of various metallic portions are so negligible than that of air gap, so that these can be easily eliminated from the model. After the removal of ground, neglected

reluctances, and bonds with zero power (due to zero effort) the reduced bond graph model is shown in Fig.6. Analysis and creation of Bond Graph model for electric field is done and potential differences as viewed from the stator and the rotor showing the poles, rotor, and frame of a three-phase, four-pole induction motor description.

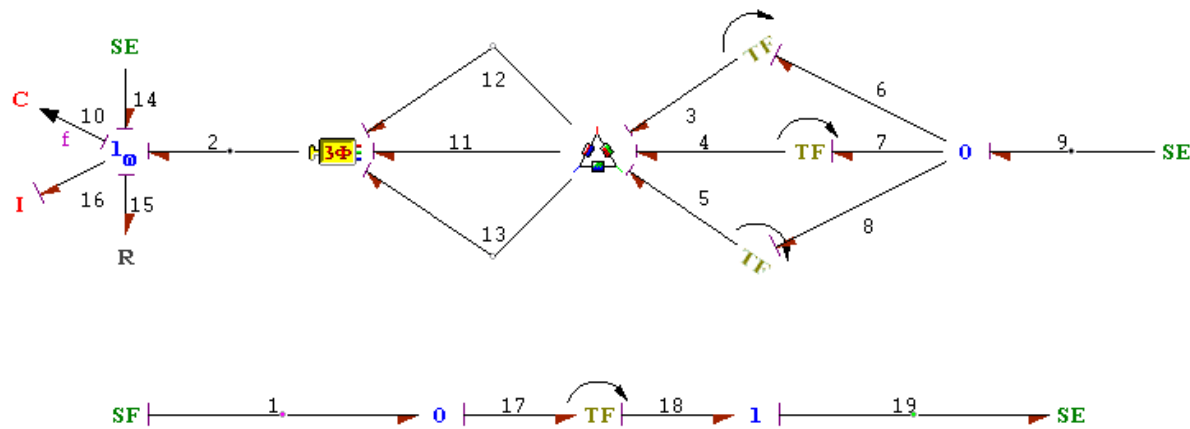


Fig. 7: Bond graph model of induction motor open loop control

## V. CONTROL OF INDUCTION MOTOR

The traditional control of DC drives are being replaced by control algorithms for induction motors from the beginning of field oriented control (FOC) of AC drives and Proportional Integral (PI) regulators, and exact feedback linearization etc. techniques from linear control theory can be used in the different control loops of the FOC scheme. Several nonlinear control techniques came into existence to overcome the above mentioned problems. Sliding mode techniques (Williams & Green, 1991; Al-Nimma & Williams, 1980; Araujo & Freitas, 2000) and artificial intelligence techniques using fuzzy logic, neuronal networks or a combination of them (Vas, 1999; Al-Nimma & Williams, 1980; Bose, 2002) are some of the modified techniques. The techniques used here is basically simple control theory with open loop control technique which leads to accurate analysis.

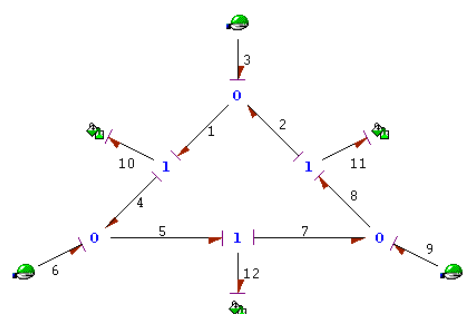


Fig.8: Bond graph Sub Model of Delta Connector

Dynamic response of the motor from the per phase equivalent circuit can be obtained as in Fig.4 above. This is similar, though not exactly same to the torque and the flux control of a dc motor. The main model as shown in the Fig.7 is a open loop control of three phase induction motor driving an inductive and a dissipative load. A three phase supply with delta starter is being provided (as shown in Fig.8 where through 3,6,9 bond effort inputs

and 10,11,12 bonds effort outputs are provided)) to drive the motor. Source of effort SE denoting the supply voltage which is connected to a 0-junction through bond 9. Connection between this 0-junction and a delta starter by three transformer with transformer (TF) function  $\cos \omega t$ ,  $\cos (\omega t-2\pi/3)$ ,  $\cos (\omega t-4\pi/3)$  through bond 3-6, 4-7, 5-8 respectively in Fig.7. Three phase induction motor as in capsule form (the bond graph model of it is shown in figure 6 above) shown in the bond graph receives power from this delta starter through three bonds 11, 12 and 13. An external load I16 and a dissipative load R15 connected at  $1_{\omega}$ -junction is being operated by the induction motor through bond 2 where a detector is placed to detect the frequency tor angular velocity. Source of flow SF connected to a 0-junction. A transformer with TF function v/f connects Source of flow SF and Source of effort SE through a 0-junction and a 1-junction. Output voltage can now be detected through a detector in bond 2. Accordingly supply voltage will have to be changed on maintain the required frequency.

With reduced supply frequency and constant rated supply voltage, tendency of the air gap flux will have a tendency to become saturated. Open loop control system finds its own equilibrium state according to controlling parameters. Motor speed or its angular position may be the desired operating equilibrium. Supply voltage or the load on the motor (controlling parameters) may or may not be under the control of the operator. With the change of the parameters such as the load or the supply voltage a new equilibrium state is reached. The stator voltage should be reduced in proportional to the frequency to maintain the air-gap flux constant. The magnitude of the stator flux is proportional to the ratio of the stator voltage and the frequency. Hence, for a fixed ratio of voltage to frequency, the flux remains constant. Also, the Developed torque remains approximately constant, by keeping V/F constant. This method gives higher run-time

efficiency. Therefore, majority of AC speed drives employ constant V/F method for the speed control.

## VI. RESULTS AND DISCUSSIONS

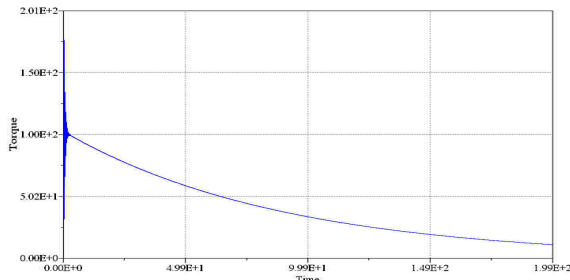


Fig.9: Torque-Time graph at no load

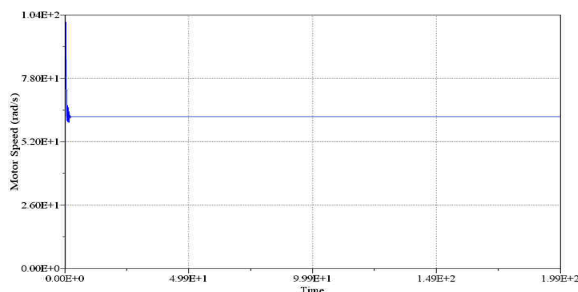


Fig.10: Speed-Time graph at no load

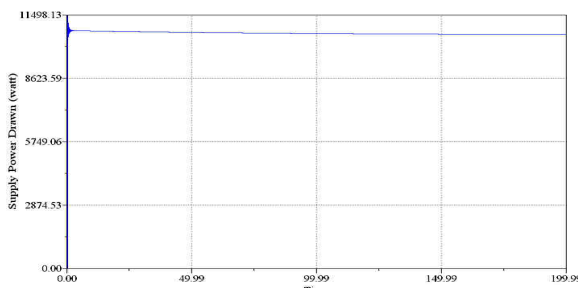


Fig.11: Supply Power Drawn at no load

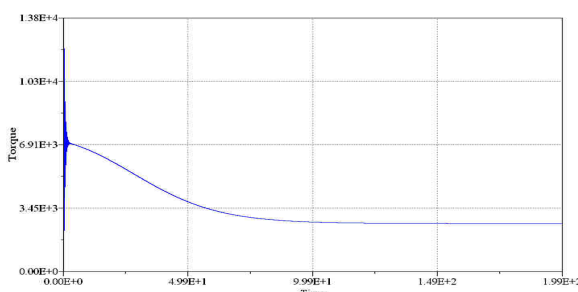


Fig.12: Torque-Time graph at on load

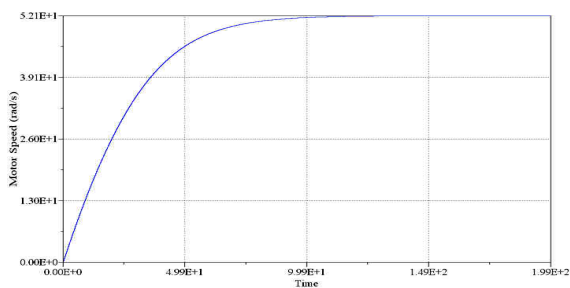


Fig.13: Speed-Time graph at on load

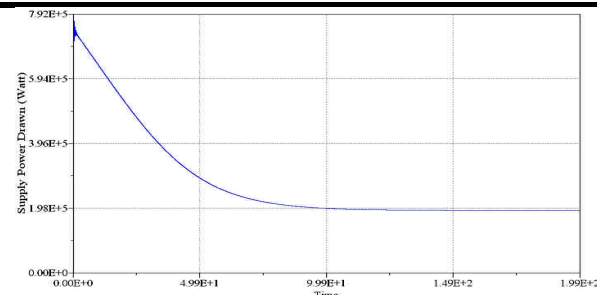


Fig.14: Supply Power Drawn at on load

## VII. CONCLUSION

Speed control of an IM by V/f control was obtained through Torque-Speed characteristics. It can be seen from the result section that with the variation of rotor resistance the starting torque can be varied and interesting conclusions can be drawn from simulation and experimental analysis whereas maximum torque remains unaffected. To obtain the maximum torque during starting for operations requiring high starting torque, the rotor resistance can be varied as per requirement and at the same time the copper losses will increase due to increase of resistance and made this method highly inefficient and impossible to use throughout the operation.

From Fig. 9 and Fig. 10 it is clear that at no-load condition and constant V/f ratio of 1 the maximum speed and supply power drawn is attained is 62.2 rad/s and 142.627 watts after 2.5 sec of transition period and the highest speed attained is 104 rad/s whereas Torque is 10.98 watts. Fig 11 depicts that a constant power is drawn 10.6 Kw at no load position. Now let's see the difference at load and by changing the V/f ratio to 8.3. Torque-time graph shows that 2610.4 N-m torque is required at on load position and this is attained after almost 100 sec of simulation and initial value is  $1.38 \times 10^4$  N-m as in Fig.12. Motor Speed at on load condition reached at 52.1 rad/sec after attaining it after transition period of almost 100 sec. Total power drawn during on load is 190.685 Kw but initially during transition period the maximum power drawn is  $7.92 \times 10^5$  Kw from the graph at Fig.14. Thus by changing the V/f ratio we can find the differences in graph and can design the induction motor for the optimum values. In this paper, an implementation and dynamic modeling of a three-phase induction motor using Bond graph are presented in a step-by-step manner and its speed control is achieved using V/f control. Using the theory of reference frames in the Bond graph environment, is a reliable and sophisticated way to analyze and predict the behavior of induction motors.

The main drawback of traditional per phase equivalent circuit analysis of an induction motor is that it is valid only for a balanced system. Erroneous analysis is required

for any imbalance in the system. Again it is impossible to obtain the dynamic response of the motor from the per phase equivalent circuit.

### NOMENCLATURE

$L_s$	stator inductance
$L_m$	mutual inductance
$L_r$	rotor inductance
$R_s$	stator resistance
$R_r$	rotor resistance
$R_{ext}$	external resistance
$v_0$	rotor speed
$P$	number of poles
$V_{ds}, V_{qs}$	d-axis and q-axis components of the stator voltage vector $V$
$V_{dr}, V_{qr}$	d-axis and q-axis components of the rotor voltage vector $V$
$i_{ds}, i_{qs}$	d-axis and q-axis components of the stator current vectors $i$
$i_{dr}, i_{qr}$	d-axis and q-axis components of the rotor current vectors $i$
$J_r$	moment of inertia of rotor
$J_L$	moment of inertia of load
$N_s$	synchronous speed in rad/sec.
$A_g$	Air gap power
H axis	angle between stator and rotor
$V_{as}; V_{bs}; V_{cs}$	stator sinusoidal phase voltages peak
$V_{ar}; V_{br}; V_{cr}$	rotor sinusoidal phase voltages
$i_{as}; i_{bs}; i_{cs}$	stator sinusoidal phase currents
$i_{ar}; i_{br}; i_{cr}$	rotor sinusoidal phase currents
$R_{as}; R_{bs}; R_{cs}$	stator winding Resistance per phase
$R_{ar}; R_{br}; R_{cr}$	rotor winding Resistance per phase
$K_{asl}; K_{bsl}; K_{csl}$	stator leakage permeance per
$K_{arl}; K_{brl}; K_{crl}$	rotor leakage permeance per
$K_m$	mutual permeance
$R_i$ resistance	core loss represented by
$N_s; N_r$	phase number of stator, rotor coils per
$K_{ss}; K_{rr}$	inductance stator- rotor per phase self

### REFERENCES

- [1] Mr. Aung Zaw Latt, Dr. Ni Ni Win," Variable Speed Drive of Single Phase Induction Motor Using Frequency Control Method", International Conference on Education Technology and Computer, 2009.
- [2] Bimal K. Bose, " Modern Power Electronics and AC Drives" Ion Boldea, S.A. Nasar," Electric Drives".
- [3] Hossein Mohktari & Abdollah Alizadeh "A New Multi-Machine Control System Based On Direct Torque Control Algorithm" pp1103-1108.
- [4] Alecsandru Simion, Leonard Livadaru and Adrian Munteanu "Mathematical Model of the Three-Phase Induction Machine for the Study of Steady-State and Transient Duty Under Balanced and Unbalanced States."
- [5] Nebojsa Mitrovic, Milutin Petronijevic, Vojkan Kostic and Borislav Jeftenic "Electrical Drives for Crane Application".
- [6] Crowder R.M. and Smith G.A. " Induction motors for crane applications" Eelectric power applications, pp 194-198 December 1979, Vol. 2, No.6.
- [7] Gan Lu ,Wang Liuping "A Multi-Model Approach to Predictive Control of Induction Motor" 978-1-61284-972-0/11/ ©2011 IEEE.
- [8] Octavian Grigore-Müller, Mihai Barbelian "The simulation of a multi-phase induction motor drive", 2010, 12th International Conference on Optimization of Electrical and Electronic Equipment, OPTIM 2010.
- [9] Li Qianxiang, Hu Jingtao, "Simulation Model of Induction Motor Based on LabVIEW", 2010 Third International Conference on Intelligent Networks and Intelligent Systems. 978-0-7695-4249-2/10 \$26.00 © 2010 IEEE , DOI 10.1109/ICINIS.2010.47.
- [10] L.Venkatesan, Dr.R.Arulmozhiyal A.D.Janarthanan, "Simulation approach on Step Speed Control of Induction Motor using Lab View", 2013 International Conference on Computer Communication and Informatics (ICCCI -2013), Jan. 04 – 06, 2013, Coimbatore, INDIA.
- [11] P. M. de la Barrera, L. I. Silva, C. H. De Angelo and G. R. Bossio, "Multi-Domain Model of Induction Motor with Stator Core Faults" pp 913-919 , 978- 1 - 4673- 0342-2112/\$31.00 ©2012 IEEE ICIT 2012.
- [12] Mukhtar Ahmad , High Performance AC Drives Modelling Analysis and Control" ISSN 1612-1287, e-ISSN 1860-4676 ,ISBN 978-3-642-13149-3 e- ISBN 978-3-642-13150-9 ,DOI 10.1007/978-3-642-13150-9. Springer London Dordrecht Heidelberg New York.
- [13] Emmanuel Delaleau, Jean-Paul Louis, Romeo Ortega, "Modeling and Control of Induction Motors", Int. J. Appl. Math. Comput. Sci., 2001, Vol.11, No.1, 105-129.
- [14] Jaroslaw Smoczek, Janusz Szpytko, "Design of Gain Scheduling Anti-Sway Crane Controller Using Genetic Fuzzy System", 978-1-4673-2124 2/12/\$31.00 ©2012 IEEE , pp573-578.
- [15] Rupak Kanti Dhar, Md. Ehtashamul Haque, Md. Alinavan Taia, Md. Ratan Sikdar, Mohammad Abdul Mannan, "Design and Simulation of Speed Control of an Induction motor Taking Core loss and Stray Load Losses Into Account" Proceedings of 2013 2nd International Conference on Advances in

Electrical Engineering (ICAEE 2013) 19-21  
December, 2013, Dhaka, Bangladesh ,pp 229-234.

- [16] Ralph Kennel, Elwy El-kholi, Sabry Mahmoud, Abdou El-refaei, Farok Elkady, “A Simple High Performance Current Control Scheme For Induction Motor Drives”, 0-7803-9252-3/05/\$20.00 ©2005 IEEE ,pp1762-1768.
- [17] Stephen L. Herman, Industrial Motor Control, 6th Edition, ISBN-13: 978-1-4354-4239-9 ISBN-10: 1-4354-4239-3, 5 Maxwell Drive Clifton Park, NY 12065-2919 USA.